

# Engineered 5S ribosomal RNAs displaying aptamers recognizing vascular endothelial growth factor and malachite green

Xing Zhang<sup>a</sup>, Ajish S. R. Potty<sup>b</sup>, George W. Jackson<sup>c</sup>, Victor Stepanov<sup>a</sup>, Andrew Tang<sup>b</sup>, Yamei Liu<sup>a</sup>, Katerina Kourentzi<sup>b</sup>, Ulrich Strych<sup>b</sup>, George E. Fox<sup>a</sup> and Richard C. Willson<sup>a,b\*</sup>

In previous work, *Vibrio proteolyticus* 5S rRNA was shown to stabilize 13–50 nucleotide “guest” RNA sequences for expression in *Escherichia coli*. The expressed chimeric RNAs accumulated to high levels in *E. coli* without being incorporated into ribosomes and without obvious effects on the host cells. In this work, we inserted sequences encoding known aptamers recognizing a protein and an organic dye into the 5S rRNA carrier and showed that aptamer function is preserved in the chimeras. A surface plasmon resonance competitive binding assay demonstrated that a vascular endothelial growth factor (VEGF) aptamer/5S rRNA chimera produced *in vitro* by transcriptional runoff could compete with a DNA aptamer for VEGF, implying binding of the growth factor by the VEGF “ribosomal RNA aptamer.” Separately, a 5S rRNA chimera displaying an aptamer known to increase the fluorescence of malachite green (MG) also enhanced MG fluorescence. Closely related control rRNA molecules showed neither activity. The MG aptamer/5S rRNA chimera, like the original MG aptamer, also increased the fluorescence of other triphenyl methane (TPM) dyes such as crystal violet, methyl violet, and brilliant green, although less effectively than with MG. These results indicate that the molecular recognition properties of aptamers are not lost when they are expressed in the context of a stable 5S rRNA carrier. Inclusion of the aptamer in a carrier may facilitate production of large quantities of RNA aptamers, and may open an approach to screening aptamer libraries *in vivo*. Copyright © 2009 John Wiley & Sons, Ltd.

**Keywords:** aptamer/5S rRNA chimera; ribosomal RNA aptamer; vascular endothelial growth factor; malachite green; aptamer; 5S rRNA scaffold; chimeric RNA

## INTRODUCTION

Aptamers—nucleic acid ligands capable of binding a pre-selected molecular target—are normally identified by *in vitro* selection from a very large pool of  $\sim 10^{15}$  randomized polynucleotides which is narrowed down to one or a few aptamers by iterative binding selection (Ellington and Szostak, 1990; Tuerk and Gold, 1990). Aptamers have been developed which bind small organic molecules (Hirao *et al.*, 1997; Babendure *et al.*, 2003; Sazani *et al.*, 2004; Chu *et al.*, 2006; Liu and Lu, 2006), proteins (Ruckman *et al.*, 1998; Jayasena, 1999; Srisawat and Engelke, 2001; Lee *et al.*, 2004), heavy metal ions (Chang *et al.*, 2005; Swearingen *et al.*, 2005; Wrzesinski and Ciesiolka, 2005; Stefan *et al.*, 2006; Wernette *et al.*, 2007) and even viruses (Gopinath *et al.*, 2006a,b). Aptamers are best known as ligands to proteins, rivaling antibodies in both affinity and specificity (Jayasena, 1999), and aptamer-based therapeutics are now emerging (Ruckman *et al.*, 1998).

Vascular endothelial growth factor (VEGF) is an essential growth factor in the early development of blood vessels. VEGF is generally not required for normal function in the adult except in wound healing, but plays an essential role in tumor growth and age-related macular degeneration (AMD). Pegaptanib sodium (Macugen; Eyetech Pharmaceuticals/Pfizer), the first aptamer drug approved for use in humans, specifically targets VEGF<sub>165</sub> and

has proven effective in treating choroidal neovascularization associated with AMD (Ng *et al.*, 2006).

Malachite green (MG), a member of the triphenyl methane (TPM) dyes, is used primarily as an antiseptic for the treatment of fungal and bacterial infections of fish in aquaculture, and as a dye in histological staining procedures. MG also has recently drawn attention as a food contaminant (Kraemer, 2008). Compared to

\* Correspondence to: R. C. Willson, Department of Chemical and Biomolecular Engineering, University of Houston, 4800 Calhoun Rd., Houston, TX 77204-4004, USA.  
E-mail: willson@uh.edu

a X. Zhang, V. Stepanov, Y. Liu, G. E. Fox, R. C. Willson  
Department of Biology and Biochemistry, University of Houston, Houston, TX, USA

b A. S. R. Potty, A. Tang, K. Kourentzi, U. Strych, R. C. Willson  
Department of Chemical and Biomolecular Engineering, University of Houston, Houston, TX, USA

c G. W. Jackson  
BioTex, Inc., Houston, TX, USA.

**Abbreviations used:** VEGF, vascular endothelial growth factor; MG, malachite green; CV, crystal violet; CAM, chicken chorioallantoic membrane; AMD, age-related macular degeneration; TPM, triphenyl methane.

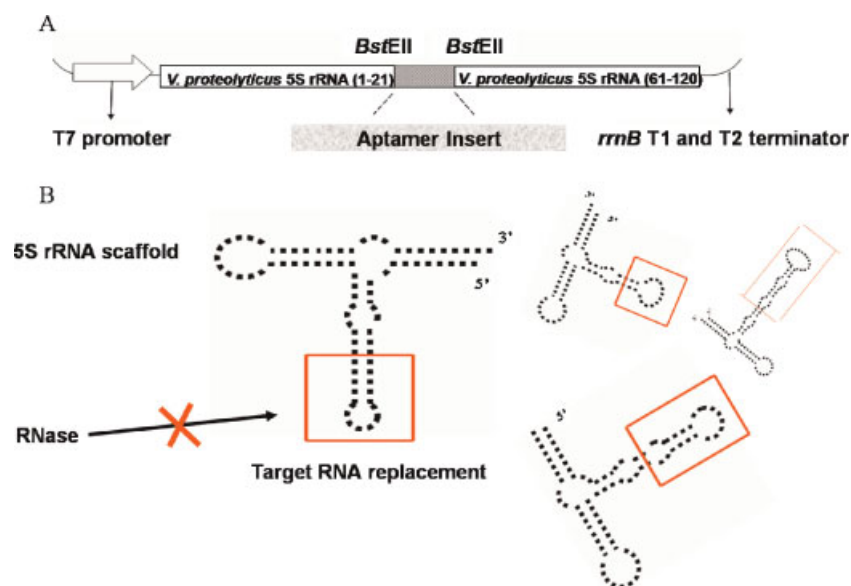


**Figure 1.** (A) Plasmid used to express aptamer/5S rRNA chimeras. The vector contains a T7 promoter, truncated 5S rRNA segments from *V. proteolyticus*, two *BstEII* sites, a T1 terminator, and a T2 terminator from the *E. coli rrnB* operon in an ampicillin-resistant backbone pCV251. (B) General schematic of expression of 5S rRNA chimeras. Target RNAs incorporated into a plasmid-encoded artificial 5S rRNA scaffold from *V. proteolyticus* are expressed under T7 control. The nucleotides in the box in the largest figure are removed from the wild-type 5S rRNA and replaced with various RNA inserts to form functional chimeras. This figure is available in color online at [www.interscience.wiley.com/journal/jmr](http://www.interscience.wiley.com/journal/jmr).

some other antiseptic agents, MG is relatively inexpensive and thus is widely used in developing countries for the treatment of bacterial and fungal infections in fish and fish eggs (Yang *et al.*, 2007). Increasing evidence, however, suggests that MG is mutagenic and carcinogenic (Mittelstaedt *et al.*, 2004). While the development of ligands and molecular sensors for MG is likely valuable in itself, for the purposes of the current study MG was chosen for its self-reporting nature when interacting with aptamer ligands. Free MG has very low quantum yield and binding of the MG aptamer used in this work greatly enhances the fluorescence of MG by stabilization of MG in a planar state (Babendure *et al.*, 2003).

Ribosomes are metabolically expensive to produce, and ribosomal RNAs, unlike mRNAs, are resistant to degradation and have long half lives (days) in the cell (Donovan and Kushner, 1986; Deana and Belasco, 2005). In our previous studies of the 5S rRNA structure space, numerous *Vibrio proteolyticus* 5S rRNA variants were produced and characterized (Hedenstierna *et al.*, 1993; Lee *et al.*, 1993, 1997; Zhang *et al.*, 2003). These included deletion mutants which did not enter the ribosomes but nevertheless accumulated to high levels in the cells (Pitulle *et al.*, 1995). One of these deletion mutants, known as the “a1 RNA” was used to create an artificial 5S rRNA vector which is strongly expressed under control of the *Escherichia coli rrnB* promoter system and terminated by *E. coli rrnB* T1 and T2 terminators (Pitulle *et al.*, 1995). Using this system, various RNA insert sequences were incorporated into the plasmid-encoded artificial 5S rRNA scaffold (Pitulle *et al.*, 1995, 1996, 1997). In each case, the expressed RNA/insert chimeras accumulated to high levels in the cell. Indeed, all members of random pools of 13- and 50-mers that were examined were stabilized to a significant extent (D’Souza *et al.*, 2003). The system has also been extended to *Pseudomonas* (D’Souza *et al.*, 2000). The expression system and a general model for expression of insert/5S rRNA chimeras are

shown in Figure 1. A similar approach has recently been introduced using tRNA as a scaffold (Ponchon and Dardel, 2007).

The aim of the present work was to construct aptamer/5S rRNA chimeras under control of the T7 promoter, and to determine whether the inserted aptamers would retain their useful properties when expressed in the context of the stable 5S rRNA carrier. Our data strongly suggest that the useful binding properties of the previously identified aptamers are not lost even when constrained by the surrounding 5S rRNA carrier. Inclusion of the aptamer in the carrier may facilitate production of large quantities of RNAs with potentially extended half-lives *in vivo*, and may open the possibility of screening aptamer libraries *in vivo* as has been done recently with small artificial mRNAs and peptides (Stepanov and Fox, 2007).

## MATERIALS AND METHODS

### Media and culture conditions

*E. coli* TG1 [*supE thi-1 Δ(lac-proAB) Δ(mcrB-hsdSM)* ( $r_{\bar{k}}^- m_{\bar{k}}^-$ ) (*F'* *traD36 proAB lacI<sup>q</sup>ZΔM15*)] was grown on Luria–Bertani (LB) broth plates or in medium with the appropriate antibiotics at 37°C. Ampicillin and kanamycin were purchased from Sigma–Aldrich (St. Louis, MO), and used at 50 and 25 μg/ml, respectively.

### Artificial 5S rRNA carrier system

A 5S rRNA-based system was established in previous work to produce artificial RNA chimeras (D’Souza *et al.*, 2000, 2003). A variant of the artificial RNA system in which a ribosomal RNA promoter was replaced by a T7 promoter was used in this work. The main elements of the artificial 5S rRNA vector (pCR21-aRNA) are as follows: a T7 promoter, a truncated 5S rRNA segment from *V. proteolyticus* with an included *BstEII* restriction site, and T1 and

**Table 1.** Aptamer and 5S rRNA chimera sequences

	Sequence 5'–3'
<i>V. proteolyticus</i> 5S rRNA (wild type)	UGCCUGGCGACCAUAGCGAUUUGGACCCACCUGAUUCCAUGCCGAACUCAGUAGUGA AACGAAUUAGCGCCGAUGGUAGUGUGGGUUUCCCAUGUGAGAGUAGGACAUCGC CAGGCAU
<i>V. proteolyticus</i> 5S rRNA with engineered <i>Bst</i> II sites and inserted identifier sequence*	UGCCUGGCGACCAUAGCGAUUGG <b>GUAACC</b> GGGUCUAGCGCUGGUUGGGUUUAA UGUGUAGUUGUUUGCCAUUUGACUGGCUG <b>GUAACCA</b> UUAGCGCCGAUGGUA GUGUGGGUUUCCCAUGUGAGAGUAGGACAUCGCCAGGCAU
Deletion mutant <i>V. proteolyticus</i> 5S rRNA	UGCCUGGCGACCAUAGCGAUUGG <b>GUAACCA</b> UUAGCGCCGAUGGUAGUGUGGG UUUCCCAUGUGAGAGUAGGACAUCGCCAGGCAU
MG RNA aptamer	GGAUCCCGACUGGCGAGAGCCAGGUAACGAAUGGAUCC
MG aptamer/5S rRNA chimera	UGCCUGGCGACCAUAGCGAUUGG <b>GUAACC</b> GGAUCCCGACUGGCGAGAGCCAGGU <u>AACGAAUGGAUCCGGUAACC</u> AAUUAGCGCCGAUGGUAGUGUGGGUUUCCCAU GUGAGAGUAGGACAUCGCCAGGCAU
VEGF RNA aptamer	GCUCAAUAGUUGGAGGCCUGUCCUCGCCGUGAGAGC
VEGF aptamer/5S rRNA chimera	UGCCUGGCGACCAUAGCGAUUGG <b>GUAACC</b> CGUCAAUAGUUGGAGGCCUGUCCU <u>CGCCGUGAGAGCGGUAACC</u> AAUUAGCGCCGAUGGUAGUGUGGGUUUCCCAU GUGAGAGUAGGACAUCGCCAGGCAU
VEGF DNA aptamer	CCGTCTTCAGACAAGAGTGCAGGG

Aptamer sequences inserted into 5S rRNA artificial cassette are underlined, and *Bst*II sites are in bold.  
\*The 53-nucleotide fragment inserted into the *Bst*II site of the engineered *V. proteolyticus* 5S rRNA is a unique identifier sequence used for non-perturbing labeling of genetically modified organisms (D'Souza *et al.*, 2000).

T2 terminators from the *E. coli* *rrnB* operon (Figure 1A). Standard recombinant DNA techniques were used to insert known VEGF- and MG-aptamer coding sequences into the artificial 5S rRNA scaffold. Agarose gel electrophoresis was used to identify candidates which appeared to have MG and VEGF aptamer coding sequences were inserted into the *Bst*II site of the vector, and positive colonies were verified by sequencing. The aptamer sequences used in this paper are summarized in Table 1. Molecular modeling of the *V. proteolyticus* 50S ribosome/ aptamer chimera was performed using Pymol (DeLano, 2002) based on PDB structure 2AW4 of the closely related *E. coli* 50S ribosome (Figure 2).

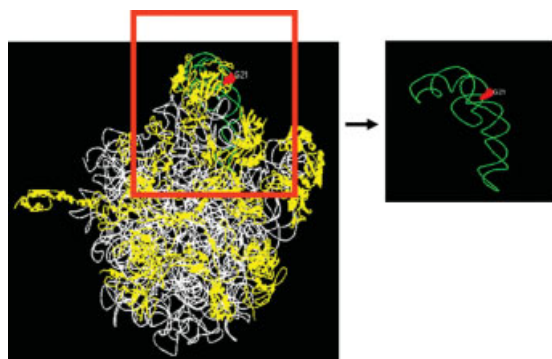


**Figure 2.** *E. coli* 50S ribosome. *V. proteolyticus* 5S rRNA shares 85% identity to *E. coli* 5S rRNA. 5S rRNA is shown in green and the insertion site for target RNAs (G21) is shown in red. 23S rRNAs is shown in white, and ribosomal proteins are shown in yellow.

### Recombinant DNA techniques

Restriction endonucleases and DNA-modifying enzymes were purchased from New England Biolabs (Ipswich, MA). Oligonucleotides for construction of VEGF and MG ribosomal RNA aptamers were purchased from Integrated DNA Technologies (Coralville, IA). DNA was annealed by denaturation at 95°C for 10 min followed by cooling to room temperature over 4 h. DNA sequencing was carried out by Lone Star Laboratories (Houston, TX).

### Bacterial expression and purification of VEGF

The human *VEGF*<sub>165</sub> gene from pET-3d-VEGF (kindly provided by Dr. Gerhard Siemeister, Tumor Biology Center, Institute of Molecular Medicine, Freiburg, Germany) was cloned into a pET-26b vector (Siemeister *et al.*, 1996). Bacterial cultures were grown to an OD<sub>600</sub> of 1.0, isopropyl-β-D-thiogalactopyranoside (IPTG) was added to a final concentration of 1 mM and the cultures were allowed to grow for another 4 h at 37°C for VEGF expression. Bacterial cells were washed in cold phosphate buffered saline (8 mM Na<sub>2</sub>HPO<sub>4</sub>; 2 mM KH<sub>2</sub>PO<sub>4</sub>; 138 mM NaCl; 2.7 mM KCl; pH 7.4), and then resuspended in chilled lysis buffer (50 mM Tris-HCl, 10 mM 2-mercaptoethanol, 2 mM EDTA, 5% glycerol, pH 8), and lysed by passage through a French Press at 10 000 psi. The mixture was centrifuged at 17 000g and 4°C for 30 min, and the pellet containing VEGF inclusion bodies was recovered. The pellet was resuspended and stirred in solubilization buffer (6 M urea, 100 mM DTT, 50 mM MES, pH 5.5) for 1 h. The solubilized mixture containing denatured VEGF was loaded onto a 40 mm internal diameter, 30 mm long SP Sepharose cation-exchange column (GE Healthcare, Piscataway, NJ). The bound VEGF eluted between 400 and 500 mM NaCl in a gradient of 100 mM to 1 M NaCl in 6 M urea over 10 column volumes.

Refolding of denatured VEGF was accomplished by mixing 20 ml of 1 mg/ml denatured VEGF with 40 ml refolding buffer (6 M urea, 0.5 M cystamine, 0.1 M glycine, 20 mM HEPES, pH 7.4) for 4 h with gentle agitation. The 60 ml mixture was then added dropwise at a flow rate of 5 ml/min to a 2 L flask containing 1140 ml of PBS with 50 mM glycine buffer, pH 7.4 with gentle stirring until the final concentrations of VEGF and urea were 50  $\mu\text{g/ml}$  and 0.3 M, respectively. The sample was centrifuged at 17 000g and 4°C for 30 min to remove aggregates. The refolded VEGF dimer was loaded on a 30 mm internal diameter and 30 mm long Heparin Sepharose 6 Fast Flow heparin-affinity column (GE Healthcare). The refolded VEGF was eluted by 40 ml of PBS/1 M NaCl, and dialyzed for 24 h against 1 L of PBS at 4°C with a Spectra/Por tubular membrane with a 6–8000 molecular weight cutoff (Spectrum Laboratories, Rancho Dominguez, CA). The concentration of VEGF was determined using the Bradford assay with bovine serum albumin (BSA) as a standard (Bradford, 1976). The final purity of VEGF was determined by SDS-PAGE (Figure 4C).

#### Characterization of the DNA aptamer binding capacity of the purified recombinant VEGF

5'-Fluorescein-labeled VEGF DNA aptamer was obtained from MWG Biotech, Inc. (High Point, NC). The association of this aptamer with our recombinant VEGF<sub>165</sub> was characterized by fluorescence anisotropy using a SPEX 212 instrument (Horiba Jobin Yvon, Edison, NJ) in T format. Fluorescein-Labeled DNA aptamer (65 nM) was titrated with VEGF (56–389 nM) in 2.5 ml PBS buffer and the change in fluorescence anisotropy was followed.

#### Chicken chorioallantoic membrane (CAM) angiogenesis assay for VEGF activity

Fertilized, specific-pathogen-free (SPF) chicken eggs were purchased from Charles River Laboratories, Inc. (Wilmington, MA). On day 1, eggs were sterilized by wiping with 70% ethanol and incubated in a Complete Hatch System incubator obtained from Double R Pet, Farm & Equestrian Supply (Palm Bay, Florida) with humidified air at 37°C. To detach the CAM from the shell, a shallow hole was made at the blunt end of a 4-day egg using a hand drill (Dremel #750 MiniMite), and 2 ml albumin was removed using an 18-gauge hypodermic needle to generate a false air sac at the top of the egg at the equator. On day 5, chicken embryo development was assessed by candling to observe growth of blood vessels. On day 6, a window was opened using fine forceps to pick away the shell over the false air sac. The window was sealed with a 4.4  $\times$  4.4 cm<sup>2</sup> sterile transparent dressing (Tegaderm<sup>TM</sup>, 3M Healthcare, St. Paul, MN). On day 11, 20  $\mu\text{l}$  of each test sample was placed on an 18  $\times$  18 mm<sup>2</sup> autoclaved glass cover slip (Baxter Healthcare Corporation, Deerfield, IL) and allowed to dry in a Class II Biosafety cabinet for 20 min. These slips were aseptically flipped over onto the CAM membranes of the eggs through the opened windows, and the windows were resealed with sterile transparent dressing. On day 14, windows were opened and angiogenesis was assayed by digital imaging of the formation of blood vessels.

#### Fluorescence enhancement assay for malachite green binding

To measure the degree of MG fluorescence enhancement by the chimeric MG aptamer/5S rRNA, RNA was added to a black 96-well

plate (Corning Life Sciences, Lowell, MA) containing 0.2 ml of 0.33  $\mu\text{M}$  MG to final RNA concentrations ranging from 0.33 nM to 3.30  $\mu\text{M}$ . All MG fluorescence measurements were performed in an EM microplate spectrofluorometer (Molecular Devices Corporation, Sunnyvale, CA). The excitation monochromator was set to either 430 or 620 nm (see below), and the emission monochromator was set to 655 nm. To minimize scattered light, a 630 nm cutoff filter was used on the emission channel. The data were analyzed using SoftMax Pro software (Version 5.0).

#### Biacore sensor assay

All surface plasmon resonance experiments were conducted at 25°C in PBS buffer with 0.005% Tween-20 using a BIAcore 2000 instrument (Biacore, Inc., Piscataway, NJ). Carboxymethylated dextran (CM5) chips were purchased from Biacore Life Sciences (Biacore, Inc.). 3'-Biotin-modified VEGF DNA aptamer (Table 1) was ordered from Integrated DNA Technologies. For sensor preparation, 3'-biotin-modified VEGF DNA aptamer was immobilized on a CM5 chip with avidin-biotin coupling chemistry as described below. Carboxymethylated dextran was activated by flowing a freshly mixed solution of 1-ethyl-3-(3-dimethylaminopropyl)-carbodiimide (EDC 400 mM) and *N*-hydroxysuccinimide (NHS 100 mM) in a 1:1 ratio over the sensor chip followed by 200  $\mu\text{l/min}$  of streptavidin for 7 min. The inactivated carboxyl groups were quenched by 1 M ethanolamine for another 7 min. A flow rate of 5  $\mu\text{l/min}$  was used throughout the procedure. The 3'-biotin-modified VEGF DNA aptamer was then bound to the streptavidin-coated sensor (on selected flow cells) at low loading densities ( $\sim$ 20 RUs) to minimize mass transport effects. This was achieved by passing 12.5 nM of the 3'-biotin-modified VEGF DNA aptamer over the chip for 2 min at 5  $\mu\text{l/min}$ . Recognition of VEGF by the aptamer/5S rRNA chimera was studied by performing a competitive binding experiment as follows: 66 nM VEGF was incubated with 300 nM VEGF-aptamer/5S rRNA chimera, or with a control RNA (*V. proteolyticus* artificial 5S rRNA or a deletion mutant *V. proteolyticus* 5S rRNA; Table 1) for 30 min. The complex was then passed over the CM5 sensor chip with immobilized biotinylated DNA aptamer to VEGF. Regeneration of the chip was achieved by treating the surface with a 10 s pulse of 2.5 mM NaOH, 25 mM NaCl with a flow rate of 40  $\mu\text{l/min}$ . Response from the reference flow cell (flow cell without the aptamer) was subtracted to get the actual response. The data were also double-referenced with blank runs of PBS buffer with 0.005% Tween-20. All runs were performed at least in duplicate. The resulting data were globally fit with parameters  $k_{\text{on}}$  (association constant;  $\text{M}^{-1} \text{s}^{-1}$ ),  $k_{\text{off}}$  (dissociation constant;  $\text{s}^{-1}$ ), and  $R_{\text{max}}$  (the maximum amount of VEGF in terms of RUs that can bind to the chip; RU) using Scrubber 2.0 (University of Utah, UT).

## RESULTS

#### Predicted secondary structures of VEGF aptamer/5S rRNA and MG aptamer/5S rRNA chimeras

Mfold (Zuker, 2003) was utilized to determine possible secondary structures of the RNA chimeras expressed from the artificial 5S rRNA vector. We expected those molecules with the lowest free energy of folding to be the most likely aptamer structures. The  $\Delta\text{G}$ 's of folding at 1 M Na<sup>+</sup> for the wild-type *V. proteolyticus* 5S

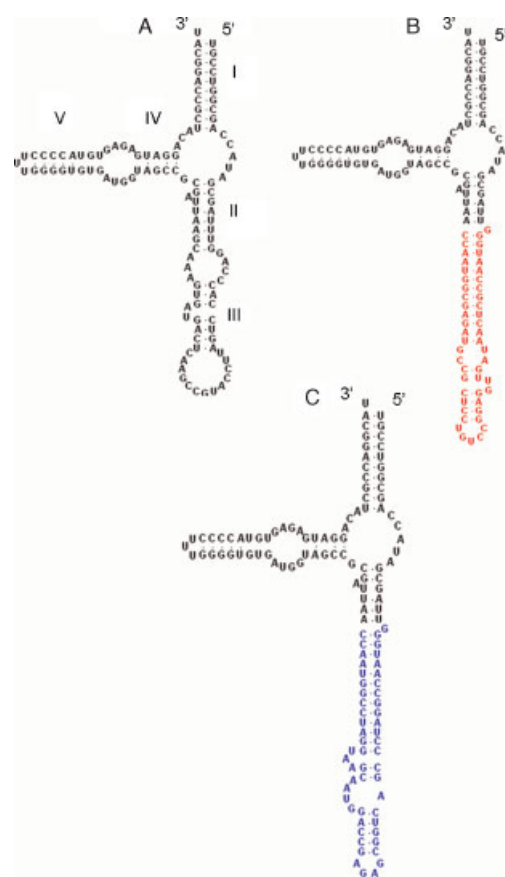


**Figure 3.** Secondary structures of RNA products from the artificial 5S rRNA vector as predicted by Mfold. (A) *V. proteolyticus* 5S rRNA complete structure. Helices are shown by roman numbers. (B) VEGF aptamer/5S rRNA chimera. The inserted VEGF aptamer and the BstEII site are shown in red. (C) MG aptamer/5S rRNA chimera. The inserted MG aptamer and the BstEII site are shown in blue. Secondary structures of the RNAs were visualized using the RnaViz 2.0 software package [Rijk *et al.*, 2003].

rRNA, VEGF-aptamer/5S rRNA chimera and MG-aptamer/5S rRNA chimeras are  $-41.4$ ,  $-57.4$ , and  $-66.1$  kcal/mol, respectively. The predicted secondary structures of the wild-type *V. proteolyticus* 5S rRNA, VEGF-aptamer/5S rRNA chimera, and MG-aptamer/5S rRNA chimeras are shown in Figure 3.

### Characterization of purified recombinant VEGF<sub>165</sub>

Denaturing cation-exchange chromatography and heparin-affinity chromatography were used to purify recombinant VEGF<sub>165</sub>. The purified VEGF<sub>165</sub> was shown by SDS-PAGE (Figure 4C) to exist as a monomer under reducing conditions at the expected molecular mass of 18 kDa, and as a dimer under non-reducing condition at the expected molecular mass of 37 kDa. Additionally, the dimer was observed by mass spectrometry at the expected molecular mass of 37 kDa (Figure 4B). To characterize the binding capacity of the purified recombinant VEGF, a fluorescein-labeled VEGF DNA aptamer and refolded, purified recombinant VEGF<sub>165</sub> were mixed and the binding was monitored by fluorescence anisotropy. The values of fluorescence anisotropy increased with the addition of purified recombinant VEGF<sub>165</sub> (from 56 to 389 nM) to a cuvette containing 65 nM fluorescein-labeled DNA aptamer in 2.5 ml PBS buffer (Figure 4A).

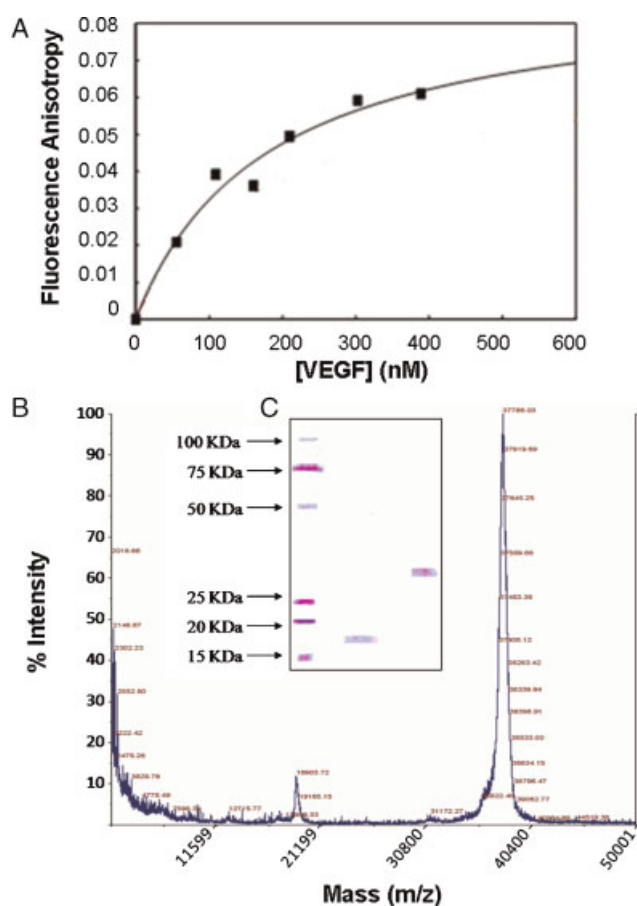


**Figure 4.** Characterization of the purified recombinant VEGF with binding assay using fluorescence anisotropy, MALDI-TOF and SDS-PAGE. (A) Fluorescence anisotropy titration of a known VEGF DNA aptamer (Table 1) with purified recombinant human VEGF<sub>165</sub>. (B) MALDI-TOF mass spectrometry of purified VEGF showing two peaks at 18 kDa (monomer) and 37 kDa (dimer). (C) SDS-PAGE analysis of the purified recombinant VEGF on a pre-cast 8-25% gradient gel using a PhastGel system. Lane 1, molecular mass markers; lane 2, Monomer form of VEGF under reducing conditions (5%  $\beta$ -mercaptoethanol); Lane 3, Dimer form of VEGF under nonreducing conditions.

These results strongly suggest that the purified recombinant human VEGF<sub>165</sub> binds to the previously identified VEGF DNA aptamer.

### Characterization of bioactivity of the purified recombinant VEGF<sub>165</sub> by chicken embryo chorioallantoic membrane (CAM) assay

An *in vivo* CAM assay was conducted to confirm the bioactivity of the refolded purified recombinant VEGF<sub>165</sub>. As shown in Figure 5, eggs treated with PBS did not show any angiogenesis (Figure 5A), but the purified recombinant human VEGF<sub>165</sub> induced dramatic angiogenesis at a concentration of 12.5  $\mu$ M (Figure 5B). A known VEGF DNA aptamer added at a concentration of 3.75 nM, greatly reduced VEGF-induced angiogenesis, presumably by direct competition for VEGF<sub>165</sub> (Figure 5C). These data demonstrate the bioactivity of the purified recombinant VEGF<sub>165</sub>, and further confirm the effectiveness of the *in vitro* refolding process.

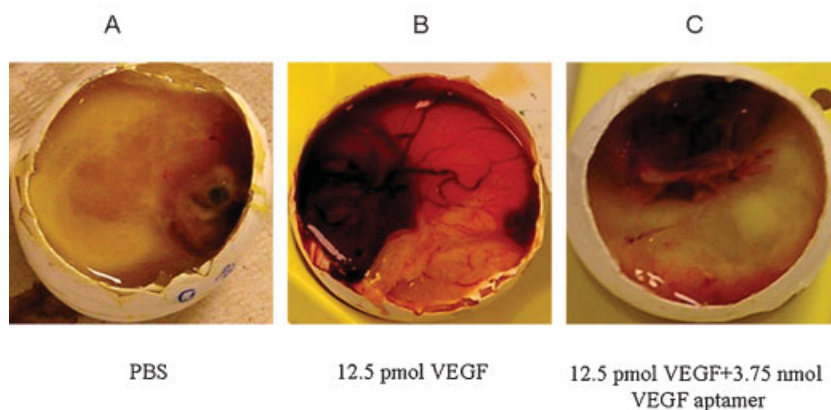


**Figure 5.** Chicken chorioallantoic membrane (CAM) angiogenic activity assay of purified refolded human VEGF<sub>165</sub>. Compared to PBS control (A), the purified VEGF caused obvious angiogenesis (B). VEGF-induced angiogenesis was inhibited by a known VEGF DNA aptamer (C).

### VEGF aptamer/5S rRNA chimera competes with a known VEGF DNA aptamer to bind VEGF

To characterize whether a VEGF-aptamer/5S rRNA chimera binds to VEGF, a competitive binding assay was conducted using surface plasmon resonance (see Materials and Methods Section) with a known VEGF DNA aptamer modified by biotin and immobilized on a streptavidin-coated M5 sensor chip. Different RNA products from the artificial 5S rRNA vector including the VEGF-aptamer/5S rRNA chimera, *V. proteolyticus* 5S rRNA and the scaffold deletion-mutant 5S rRNA were pre-incubated with 65 nM of VEGF for 30 min at room temperature. The pre-associated complexes were then applied to the immobilized VEGF DNA aptamer chip. It was anticipated that if the recognition properties of the VEGF-aptamer/5S rRNA chimera were retained, it would compete with the immobilized DNA aptamer for binding to VEGF, reducing the SPR response of the DNA/VEGF interaction in the presence of the chimeric RNA. Figure 6 illustrates the binding of VEGF (66 nM), and the preformed complexes of VEGF (66 nM) to the scaffold deletion mutant 5S rRNA (900  $\mu$ M), wild-type *V. proteolyticus* 5S rRNA (300  $\mu$ M), and of the VEGF-aptamer/5S rRNA chimera (300  $\mu$ M) to the immobilized DNA aptamer. Visual

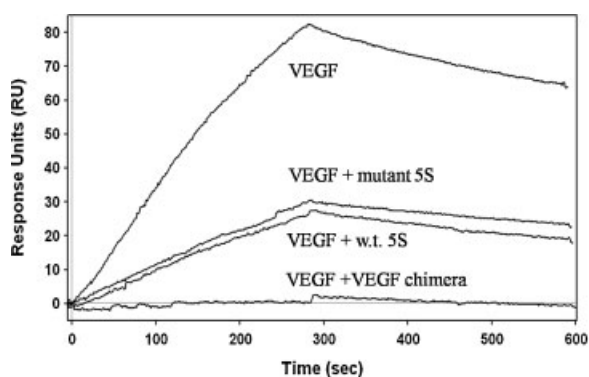


**Figure 6.** Surface plasmon resonance competition assay of VEGF aptamer/5S rRNA chimera and a known VEGF DNA aptamer for VEGF using a Biacore 2000. Immobilized DNA aptamer competed for human VEGF<sub>165</sub> (66 nM) in preformed complexes with truncated mutant 5S rRNA (900  $\mu$ M), wild-type 5S rRNA (300  $\mu$ M), and VEGF aptamer/5S rRNA chimera (300  $\mu$ M).

inspection of the competitive binding sensorgrams clearly shows that the VEGF chimera completely sequesters VEGF; however, the controls also bind to VEGF to some extent (Figure 6). A quantitative analysis of these sensorgrams indicated that the VEGF chimera completely binds to VEGF, resulting in a flat response line due to the non-availability of VEGF for the immobilized aptamer. The controls, deletion mutant 5S rRNA and wild-type 5S rRNA, bind 73% of the VEGF offered for binding, leaving only 27% of VEGF available for the immobilized DNA aptamer. This non-specific binding could be attributed to long-range electrostatic interactions of positively charged VEGF with polyanionic RNA and template plasmid.

### MG-aptamer/5S rRNA chimera binds to malachite green and enhances fluorescence of the dye

It has been reported that free MG has low fluorescence while in a vibrationally free state (Babendure *et al.*, 2003). The binding of MG aptamer to free MG fixes MG in a planar state, dramatically increasing MG fluorescence yield. To determine whether the MG aptamer maintained the ability to recognize MG while constrained by the surrounding 5S rRNA scaffold, MG fluorescence was monitored during titration with MG-aptamer/5S rRNA chimeric RNA. As shown in Figure 7, the MG aptamer/5S rRNA chimera increased MG fluorescence dramatically while *V. proteolyticus* 5S rRNA and controls did not. Not surprisingly, we were also able to see increased fluorescence of *E. coli* cell cultures expressing the MG aptamer in medium containing MG; this enhancement was not seen with control strains (data not shown). Our results strongly suggest that, like the VEGF aptamer, the MG aptamer maintains its target recognition functionality even within the context of the *V. proteolyticus* 5S rRNA scaffold.

Furthermore, the MG-aptamer/5S rRNA chimera shows MG affinity ( $K_d$  900 nM) similar to that of the free MG aptamer [ $K_d$  1000 nM in this work, 800 nM reported previously (Baugh *et al.*, 2000)]. The related TPM dye Crystal Violet (CV) bound more weakly to the 5S/aptamer chimera with a  $K_d$  of 107  $\mu$ M and to the original MG aptamer with a  $K_d$  of 122  $\mu$ M confirming that the 5S chimera displays at least some aspects of the specificity of the original aptamer, in addition to its MG affinity. The chimera bound to each of these dyes (and to the related dye methyl violet, results not shown) with slightly higher affinity than the parent aptamer, raising the possibility that suppression of conformational entropy

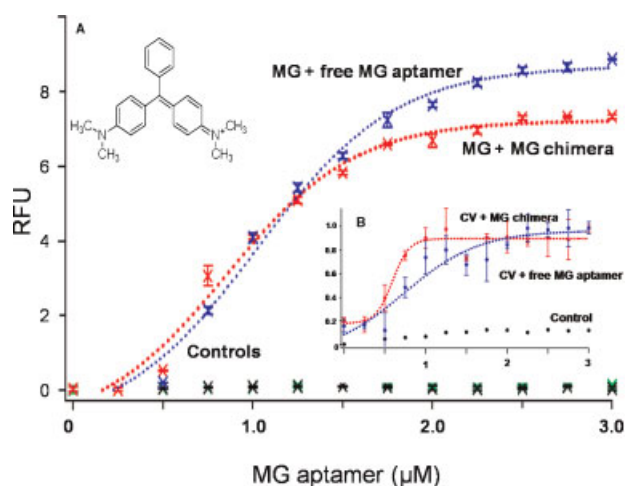


**Figure 7.** MG aptamer/5S rRNA chimera enhances fluorescence of malachite green and crystal violet. Malachite green and crystal violet (0.33  $\mu\text{M}$ ) were incubated with 5S rRNA/MG aptamer chimera, free MG aptamer or wild-type 5S rRNA (control) for 10 min at room temperature. Fluorescence of the complex was measured by a Gemini EM microplate spectrofluorometer. Each value represents the mean  $\pm$  standard deviation for three replicates. The best fit was determined using Igor Pro 4.04 (WaveMetrics, Inc., Portland, OR). (A) MG: excitation wavelength 430 nm; emission 655 nm; cutoff 630 nm. (B) CV: excitation 570 nm; emission 650 nm; cutoff 630 nm. This figure is available in color online at [www.interscience.wiley.com/journal/jmrm](http://www.interscience.wiley.com/journal/jmrm).

of the aptamer increases affinity in the chimera, but this possibility requires further investigation.

## DISCUSSION

In this paper, we proposed a novel expression system for RNA aptamers in *E. coli* using a 5S rRNA scaffold. Our results demonstrate that both VEGF and MG RNA aptamers retain their useful recognition properties even when constrained by the 5S rRNA scaffold. As mentioned above, MG as an aptamer target is interesting for a variety of reasons but was chosen in this study primarily due to its self-reporting fluorescence enhancement upon binding to previously described aptamers. Using this feature, it has been shown here that an MG aptamer retains recognition for the target dye molecule with sensitivity and specificity despite being conformationally constrained at both the 5'- and 3'-ends and despite any additional steric hindrance resulting from the 5S rRNA derived scaffold. As shown in Figure 7, MG can be readily detected *in vitro* at concentrations as low as 0.33  $\mu\text{M}$  with MG aptamer/5S rRNA chimera.

Aside from the sensing application, it is known that MG has three different forms including chromatic MG, carbinol base, and leuco MG. Chromatic MG is the most commonly known form with a characteristic green color and can be converted to carbinol base and leuco MG through cell metabolism. Among them, leuco MG is believed to be most toxic to humans (Mittelstaedt *et al.*, 2004). A method to prevent the conversion of chromatic MG to leuco MG might be important for prophylaxis following MG exposure or ingestion. As both MG aptamer and MG aptamer/5S rRNA chimera firmly bind to MG, it is tempting to speculate that they could be used to sequester MG and block the conversion from chromatic MG to leuco MG. Further work would be needed to test this hypothesis.

The low yield and high costs of *in vitro* transcription or chemical synthesis of RNA at large scales (i.e., for RNA as a pharmaceutical) are quite burdensome. In this paper, we constructed an aptamer/5S rRNA expression system which may offer a promising approach to expression and production of functional RNA aptamers at a large scale by conventional fermentation of *E. coli*. While non-natural modifications could not be directly introduced via fermentation, we have shown previously with non-aptamer RNAs that by "camouflaging" the desired RNA within a scaffold resembling 5S rRNA, the aptamer product(s) should exhibit enhanced stability to nuclease degradation. In this work in particular, we have clearly demonstrated that a 5S-MG aptamer RNA retains its ability to bind MG even after prolonged storage of the cells. Of course, in addition to the large-scale production of chimeric ribosomal aptamers, our approach may be useful for the insertion of a number of other functional RNAs within an rRNA scaffold including siRNAs, microRNAs, ribozymes, etc. As we have previously shown, the 5S rRNA deletion construct can readily host RNA inserts up to 120 nt (D'Souza *et al.*, 2003) such that inserts with dual function may be generated (e.g., an aptamer conjugated to an siRNA). Finally, based on the demonstration here that aptamers identified *a priori* can be inserted in our 5S rRNA-based system without loss of functionality, we have initiated studies on *in vivo* selection of aptamers starting with randomized inserts and appropriate selection pressure.

## Acknowledgements

We thank the members of the Willson and Fox laboratories for helpful discussions. This work was supported by NIH and by grants from the Robert A. Welch Foundation (E-1264 and E-1451) as well as NIH STTR grant 1R41ES016478 to GWJ in collaboration with GEF and RCW.

## REFERENCES

- Babender JR, Adams SR, Tsien RY. 2003. Aptamers switch on fluorescence of triphenylmethane dyes. *J. Am. Chem. Soc.* **125**: 14716–14717.
- Baugh C, Grate D, Wilson C. 2000. 2.8 Å crystal structure of the malachite green aptamer. *J. Mol. Biol.* **301**: 117–128.
- Bradford MM. 1976. A rapid and sensitive method for the quantitation of microgram quantities of protein utilizing the principle of protein-dye binding. *Anal. Biochem.* **72**: 248–254.
- Chang I-H, Tulock J, Liu J, Kim W-S, Cannon D Jr, Lu Y, Bohn P, Sweedler J, Cropek D. 2005. Miniaturized lead sensor based on lead-specific DNzyme in a nanocapillary interconnected microfluidic device. *Environ. Sci. Technol.* **39**: 3756.
- Chu TC, Marks 3rd JW, Lavery LA, Faulkner S, Rosenblum MG, Ellington AD, Levy M. 2006. Aptamer:toxin conjugates that specifically target prostate tumor cells. *Cancer Res.* **66**: 5989–5992.

- Deana A, Belasco JG. 2005. Lost in translation: The influence of ribosomes on bacterial mRNA decay. *Genes Dev.* **19**: 2526–2533.
- D'Souza LM, Willson RC, Fox GE. 2000. Expression of marker RNAs in *Pseudomonas putida*. *Curr. Microbiol.* **40**: 91–95.
- D'Souza LM, Larios-Sanz M, Setterquist RA, Willson RC, Fox GE. 2003. Small RNA sequences are readily stabilized by inclusion in a carrier rRNA. *Biotechnol. Prog.* **19**: 734–738.
- DeLano WL. 2002. The PyMOL User's Manual. DeLano Scientific: Palo Alto, CA, USA.
- Donovan WP, Kushner SR. 1986. Polynucleotide phosphorylase and ribonuclease II are required for cell viability and mRNA turnover in *Escherichia coli* K-12. *Proc. Natl. Acad. Sci. USA* **83**: 120–124.
- Ellington AD, Szostak JW. 1990. In vitro selection of RNA molecules that bind specific ligands. *Nature* **346**: 818–822.
- Gopinath SCB, Misono TS, Kawasaki K, Mizuno T, Imai M, Odagiri T, Kumar PKR. 2006a. An RNA aptamer that distinguishes between closely related human influenza viruses and inhibits haemagglutinin-mediated membrane fusion. *J. Gen. Virol.* **87**: 479–487.
- Gopinath SCB, Sakamaki Y, Kawasaki K, Kumar PKR. 2006b. An efficient RNA aptamer against human influenza B virus hemagglutinin. *J. Biochem.* **139**: 837–846.
- Hedenstierna KO, Lee YH, Yang Y, Fox GE. 1993. A prototype stable RNA identification cassette for monitoring plasmids of genetically engineered microorganisms. *Syst. Appl. Microbiol.* **16**: 280–286.
- Hirao I, Yoshinari S, Yokoyama S, Endo Y, Ellington AD. 1997. In vitro selection of aptamers that bind to ribosome-inactivating toxins. *Nucleic Acids Symp. Ser.* **37**: 283–284.
- Jayasena SD. 1999. Aptamers: An emerging class of molecules that rival antibodies in diagnostics. *Clin. Chem.* **45**: 1628–1650.
- Kraemer D. 2008. Hearing on Chinese Seafood: Safety and Trade Issues: "U.S.-China Economic and Security Review Commission". FDA: Washington, D.C.; <http://www.fda.gov/ola/2008/seafood042408.html>.
- Lee YH, D'Souza LM, Fox GE. 1993. Experimental investigation of an RNA sequence space. *Orig. Life Evol. Biosphere* **23**: 365–372.
- Lee YH, D'Souza LM, Fox GE. 1997. Equally parsimonious pathways through an RNA sequence space are not equally likely. *J. Mol. Evol.* **45**: 278–284.
- Lee JF, Hesselberth JR, Meyers LA, Ellington AD. 2004. Aptamer database. *Nucleic Acids Res.* **32**: D95–D100.
- Liu J, Lu Y. 2006. Fast colorimetric sensing of adenosine and cocaine based on a general sensor design involving aptamers and nanoparticles. *Angew. Chem. Int. Ed.* **117**: 90–94.
- Mittelstaedt RA, Mei N, Webb PJ, Shaddock JG, Dobrovolsky VN, McGarrity LJ, Morris SM, Chen T, Beland FA, Greenlees KJ, Heflich RH. 2004. Genotoxicity of malachite green and leucomalachite green in female Big Blue B6C3F1 mice. *Mutat. Res.* **561**: 127–138.
- Ng EW, Shima DT, Calias P, Cunningham ET Jr, Guyer DR, Adamis AP. 2006. Pegaptanib, a targeted anti-VEGF aptamer for ocular vascular disease. *Nat. Rev. Drug Discov.* **5**: 123–132.
- Pitulle C, D'Souza L, Fox GE. 1997. A low molecular weight artificial RNA of unique size with multiple probe target regions. *Syst. Appl. Microbiol.* **20**: 133–136.
- Pitulle C, Hedenstierna KO, Fox GE. 1995. A novel approach for monitoring genetically engineered microorganisms by using artificial, stable RNAs. *Appl. Environ. Microbiol.* **61**: 3661–3666.
- Pitulle C, Hedenstierna KOF, Fox GE. 1996. Useful properties of restriction enzymes that recognize interrupted palindromes. *Biotechniques* **21**: 619–622.
- Ponchon L, Dardel F. 2007. Recombinant RNA technology: The tRNA scaffold. *Nat. Methods* **4**: 571–576.
- Rijk PD, Wuyts J, Wachter RD. 2003. RnaViz2: An improved representation of RNA secondary structure. *Bioinformatics* **19**: 299–300.
- Ruckman J, Green LS, Beeson J, Waugh S, Gillette WL, Henninger DD, Claesson-Welsh L, Janjic N. 1998. 2'-Fluoropyrimidine RNA-based aptamers to the 165-amino acid form of vascular endothelial growth factor (VEGF165), inhibition of receptor binding and Vegf-induced vascular permeability through interactions requiring the Exon 7-encoded domain. *J. Biol. Chem.* **273**: 20556–20557.
- Sazani PL, Larralde R, Szostak JW. 2004. A small aptamer with strong and specific recognition of the triphosphate of ATP. *J. Am. Chem. Soc.* **126**: 8371.
- Siemeister G, Schnurr B, Mohrs K, Schachtele C, Marme D, Martiny-Baron G. 1996. Expression of biologically active isoforms of the tumor angiogenesis factor VEGF in *Escherichia coli*. *Biochem. Biophys. Res. Commun.* **222**: 249–2455.
- Srisawat C, Engelke DR. 2001. Streptavidin aptamers: Affinity tags for the study of RNAs and ribonucleoproteins. *RNA* **7**: 632–641.
- Stefan LR, Zhang R, Levitan AG, Hendrix DK, Brenner SE, Holbrook SR. 2006. MeRNA: A database of metal ion binding sites in RNA structures. *Nucleic Acids Res.* **34**: D131–D134.
- Stepanov VG, Fox GE. 2007. Stress-driven in vivo selection of a functional mini-gene from a randomized DNA library expressing combinatorial peptides in *Escherichia coli*. *Mol. Biol. Evol.* **24**: 1480–1491.
- Swearingen CB, Wernette DP, Cropek DM, Lu Y, Sweedler JV, Bohn PW. 2005. Immobilization of a catalytic DNA molecular beacon on Au for Pb(II) detection. *Anal. Chem.* **77**: 442–448.
- Tuerk C, Gold L. 1990. Systematic evolution of ligands by exponential enrichment: RNA ligands to bacteriophage T4 DNA polymerase. *Science* **249**: 505–510.
- Wernette DP, Kim H-K, Liu J, Swearingen CB, Yue Z, Zavareh M, Ingram CW, Economy J, Shannon MA, Bohn PW, Lua Y. 2007. New catalytic DNA biosensors for trace contaminants in water: "Water CampWS." [http://www.watercampws.uiuc.edu/media/uploads/research\\_posters/wernette\\_et\\_al\\_-\\_dna\\_biosensors.20070205.45c7a063e298c6.54566625.pdf](http://www.watercampws.uiuc.edu/media/uploads/research_posters/wernette_et_al_-_dna_biosensors.20070205.45c7a063e298c6.54566625.pdf).
- Wrzesinski J, Ciesiolka J. 2005. Characterization of structure and metal ions specificity of Co<sup>2+</sup>-binding RNA aptamers. *Biochemistry* **44**: 6257–6268.
- Yang MC, Fang JM, Kuo TF, Wang DM, Huang YL, Liu LY, Chen PH, Chang TH. 2007. Production of antibodies for selective detection of malachite green and the related triphenylmethane dyes in fish and fishpond water. *J. Agric. Food Chem.* **55**: 8851–8856.
- Zhang Z, D'Souza LM, Lee YH, Fox GE. 2003. Common 5S rRNA variants are likely to be accepted in many sequence contexts. *J. Mol. Evol.* **56**: 69–76.
- Zuker M. 2003. Mfold web server for nucleic acid folding and hybridization prediction. *Nucleic Acids Res.* **31**: 3406–3415.